2. MODELLING OF GEOLOGICAL HAZARDS AND RESOURCES

2.1 SISME: South Indian Strain Measurement Experiment

Six new GPS points were established in the Southern Indian Peninsula, thereby raising the total number to 24. Measurements were made at 11 stations of these points forming 17 baselines Fig 2.1. Data was processed using the Bernese Software with the IISC point as reference whose co-ordinates were estimated in the International Terrestrial Reference Frame (ITRF94). Repeatabilities in the baseline determinations so obtained are up to 5 mm in the east and up to 9mm in the North.

Comparison of Baselines IISC-CHEN and IISC-PONN using the of 1994, 1995 and 1996 data indicate extension of baselines at the rate of 0.018 and 0.015 mm/km/yr. respectively. This was compared with a model of an elastic plate subjected to an end load (Himalaya) which shows zones of tension and compression along the plate from Himalaya to Kanyakumari. These results suggest buckling/basin formation in the Indian plate. (*V.Kumar, G.K.Sharma, J.Paul, V.K.Gaur and R.N.Singh*)

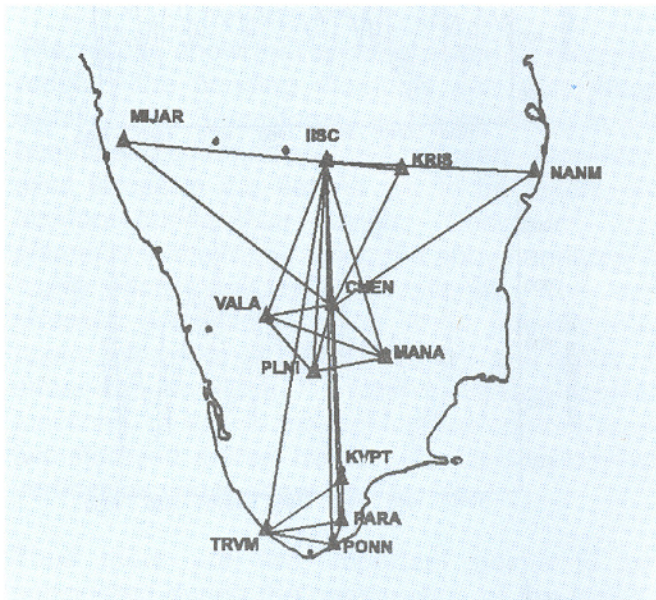

Fig 2.1: GPS stations and Baselines measured in South Indian Peninsula during Sept 1996.

2.2 Strain Measurement Studies in the Himalaya Using GPS

The rate of collision between the India sub-continent and Southern Tibet determines the recurrence interval of great earthquakes beneath the Himalaya. Baseline determination between some points in the Himalaya and those south of it were accordingly made to quantify the kinematics of deformation of the Garhwal-Kumaon Himalaya. GPS measurements were initiated at 10 stations (Sukhi, Chamba, Lansdowne, Pauri, Tungnath, Auli, Almora, Khoont, Chaukiri and Munsiyari, see Fig. 2.2) so as to obtain a good spread across the Garhwal and Kumaon region of the Himalaya. Measurement were carried for three days at each station for duration of 24hr each day. Processing of the data using Bernese software is in progress. Data processed so far yielded repeatabilities of up to 3mm in the east and up to 8mm in the north. (*J.Paul, G.K.Sharma, V.Kumar, V.K.Gaur*)

2.3 Indian Plate Motion and Convergence Across the Lesser Himalaya

GPS data acquired from 1991 to 1995 were used to constrain the motion of sites in Bangalore in southern India, and Kathmandu, Nepal, relative to a global GPS network. These measurements

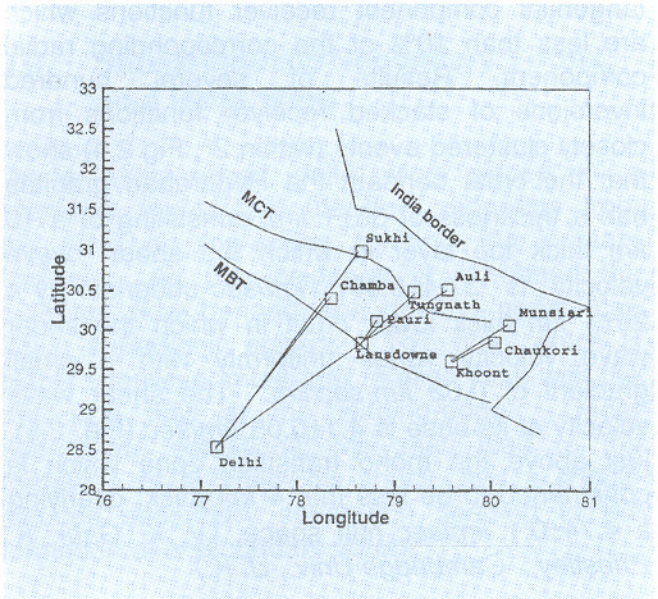

Fig 2.2: GPS stations and Baselines measured in Garhwal and Kumaon Himalaya during Oct - Nov 1996.

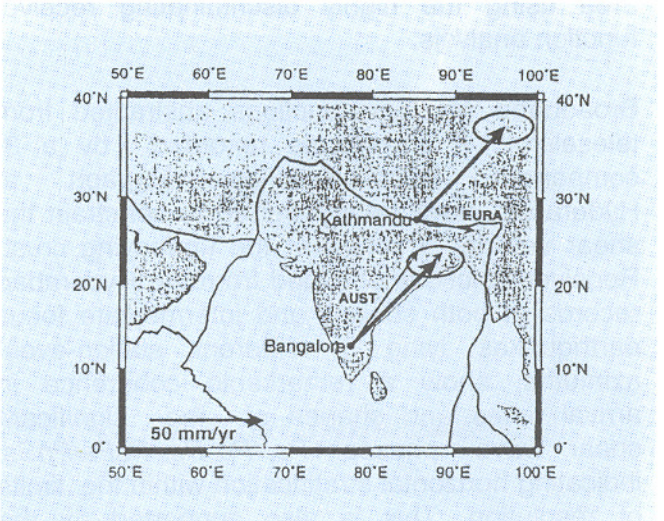

Fig 2.3: Measured site velocities between 1991 and 1995 and their 95% confidence ellipses in the ITRF92 reference frame. The GPS results are compared to the NNR-NUVEL-1A plate-motion model (thin for the Indian and Australian plates are shown; the Indian plate result is very close to the observed velocity. For Kathmandu, the predictions for the Indian and Eurasian plates are shown; the Indian plate prediction is obscured by the data vector.

permit estimates of the northward motion of the Indian plate and convergence between the southern Himalaya and the Indian subcontinent. The velocities of Bangalore and Kathmandu in the ITRF92 reference frame were 38 ± 5 in the East ; 38 ± 3 in the North and 38 ± 5 in the East ; 42 ± 3 in the North respectively (Fig 2.3) and agree with that predicted by the NNR-NUVEL1A plate motion model for the Indian plate motion, and differ from that predicted for the Australian plate, confirming the independent motion of the Indian and Australian plate fragments. No significant motion was detected between Bangalore and Kathmandu during the three years from 1991-1994, even though Kathmandu is located in the hanging wall of the active Himalayan thrust system. The Himalayan thrust system is thought to accommodate 18 ± 7 mm/yr. of convergence and has been the source of several historic M ≈ 8 earthquakes. The absence of motion of Kathmandu relative to the Indian plate can be explained if the thrust system is presently locked south of Greater Himalaya. Our preferred model has no steady slip on the detachment south of the greater Himalaya, and steady slip at a rate greater than 6 mm/yr. (1/3 of the long-term convergence rate) can be ruled out at 95% confidence level. (*J.Paul, Sridevi Jade, V.K.Gaur, V.Kumar, G.K.Sharma, J.Freymueller, R.Bilham, R.Burgmann, K.Larson,* US Collaborators)

2.4 Shear Wave Velocity Structure Beneath the Archean Granites Around Hyderabad

Hyderabad (17-417°N, 78.55°E) is located on the Archaean granite terrain of the Sourthern Indian craton. These granites have a Rb-Sr age of 2600 Ma, and are dominated by alkali feldspars (potassic) unlike the tonalitic (sodic) granites of the country further south in Karnataka. The granitization process that created such a large volume of batholithic-proportion potassium enriched rocks, remains a mystery and although several studies have led to estimates of the gross crustal properties, there is little definitive evidence regarding the nature of their finer structure. The recent availability of 3-component broadband seismic records from the GROSCOPE station at NGRI, Hyderabad (HYB) however, presented a new opportunity for investigating the fine scale structure beneath the

area using the highly discriminating receiver function analysis.

Broadband receiver functions abstracted from teleseismic *P* waveforms recorded by a 3-component Streckeisen seismograph at Hyderabad, have been inverted to constrain the shear velocity structure of the underlying crust. Receiver functions obtained from the Hyderabad records of both shallow and intermediate focus earthquakes lying in different station-event azimuths, show a remarkable coherence in arrival times and shapes of the significant shear wave phases: *Ps, Pp Ps, PsPs/PpSs,* indicating horizontal stratification within the limits of resolution. This is also supported by the relatively small observed amplitudes of the tangential component receiver functions which are less than 10% of the corresponding radial component. Results of several hundred inversions of stacked receiver functions from closely clustered events (within 2°, Fig 2.4) show that the crust beneath the Hyderabad granites has a thickness of 36±1 *km*, consisting of a 10 *km* thick top layer in which the shear wave velocity is 3.54±0.007 *km/sec* underlain by a 26±1 *km* thick lower crust in which the shear wave velocity varies uniformly with a small gradient of 0.02 *km/sec/km.* The shear wave velocity at its base is 4.1±0.05 *km/sec* (Fig. 2.5), just above the moho transition zone which is constrained to be less that 4 *km* thick, overlying a 4.74±0.1 *km/sec* half space. *(V. K. Gaur, K. Priestley*, *Cambridge Univ., U. K.)*

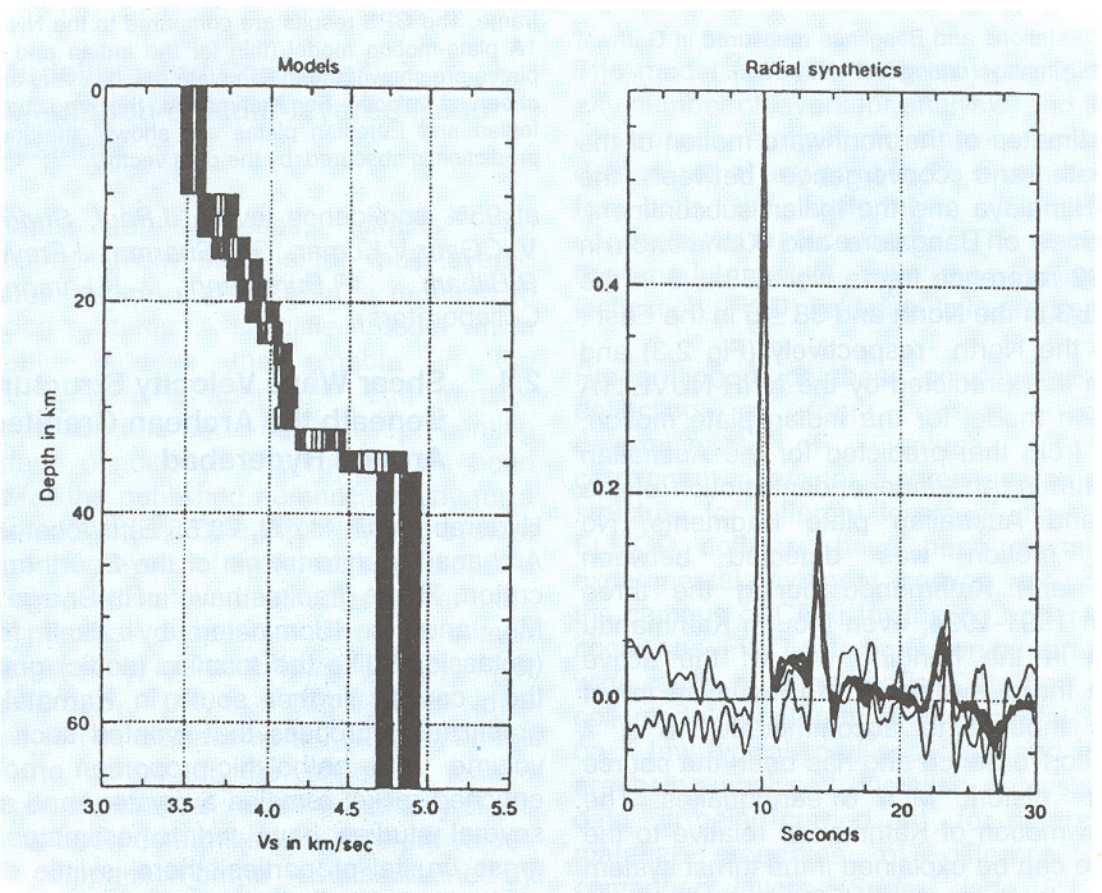

Fig. 2.4: (a) Final crustal models from the simultaneous inversion of the two radial receiver functions.
(b) The fit of the resulting model synthetic radial receiver functions to the ± one standard deviation bounds.

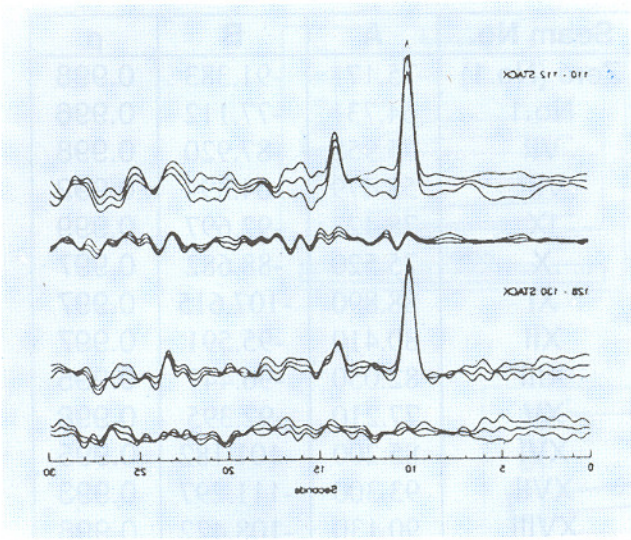

Fig. 2.5: Comparison of two radial (the upper waveform in each) and tangential receiver function stacks used in the simultaneous inversion for the crustal structure beneath HYB.

2.5 Bioremediation

Contamination of soil and ground water in the oil fields of Assam is a problem to be tackled on an urgent basis due to the extent of the problem. For example, many of the oil fields have been in operation for a while now and leakages and spillages of crude oil are a common phenomenon during routine operations. Depending on the site location, the level of oil contaminant with soil may be as high as 10% W/W. Bioremediation is a process which exploits the ability of natural micro-organisms to degrade organic contaminant in soil and ground water. It has the advantage that it can be employed *in situ* and has been also shown to be a technology capable of achieving permanent remediation at waste sites.

Designing field efficient methods of implementing this technology has been taken up as a joint venture with Regional Research Laboratory, Jorhat. Laboratory trials take up periods of the order of months and hence modelling and simulation come in useful to test out the sensitivities to different parameters of the problem. We had reported last year on the software package developed at C-MMACS for the simulation runs. Results of some of the experimental runs conducted at RRL are available now. The results (see Fig. 2.6) are in conformity with the simulation predictions which were reported last year. For example, nutrient addition under aerated conditions have been shown to increase the rate of biodegradation. Extraneous microbial consortia does not provide any extra advantages implying that the biodegradation capability of the indigenous micro-organisms is adequate for the process. Based on these results, parameter initialisations have been possible with reference to the specific site conditions. Simulations are now under way to generate opimal scenarios based on these initialisations. The simulations are, in particular, geared to tackle the high initial concentrations which are a significant site specific feature of the problem. *(T. R. Krishnamohan)*

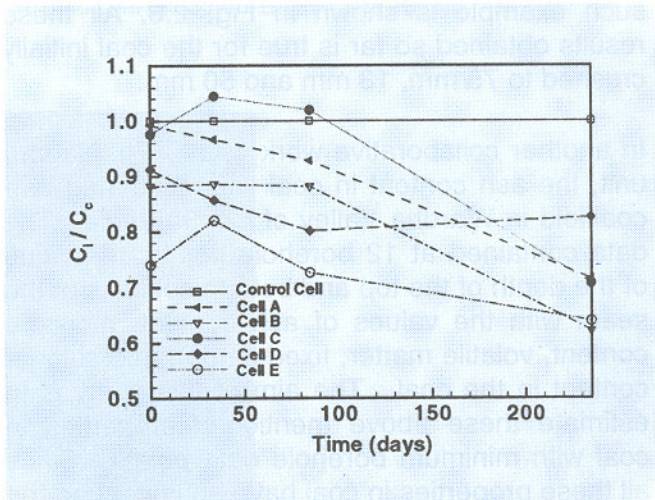

Fig. 2.6 Ratio of oil concentration in the appropriate cell (C_i) to the oil concentration in the control cell (C_c) is plotted against time. The cells A-E differs from the control cell in that Cell A has nutrient added, Cell B has nutrient + Consortium + Air, Cell C has nutrient + Consortium, Cell D has nutrient + air and Cell E has no nutrient but air is supplied. These experimental results are from a batch of experiments conducted at RRL, Jorhat.

2. 6 Ash Distribution in Coal

In continuation with the work done during 1995-1996, for the estimation of ash content in coal, further analysis was carried out on the data provided by CFRI on coal yield and ash content

in different seams. It was found that the analysis of the data for different sections in a seam does not show any changes. Therefore each seam is studied separately for their ash and yield distribution with respect to the specific gravity and size fractions. It was found that all the seams show a maximum yield of coal when processed in a liquid with specific gravity between 1.5 and 1.6 except the seams VII and VIII. For all the seams the ash content versus specific gravity fits linear. Table 2.1 gives the values of the parameters A and B for the fit $a = A+B\rho$ with respective correlation values, where a is the ash content and ρ is the specific gravity.

It is also seen that the size reduction does not effect the ash content in different seams. One such example is shown in Fig. 2.6. All these results obtained so far is true for the coal initially crushed to 75 mm, 13 mm and 50 mm.

In another collaborative work with CFRI, Nagpur unit, the ash content in coal was estimated in a coalfield in Wardha Valley of Central India. The data contained at 12 borehole points, the value of the depth of the top and bottom sections of the seam with the values of ash content, moisture content, volatile matter, fixed carbon and sulphur content in the coal. The aim of this study is to estimate these above mentioned properties in coal with minimum borehole data points. Since all these properties in coal have an impact on the environment, it is essential to estimate the quantity of each of these present is a coalfield with minimum expenditure by minimizing the number of boreholes. As an exercise to start with, the values sulphur content in the coalfield was considered. A 2-D interpolation technique was employed to identify the contours of sulphur content and their pattern when all the points are

Seam No.	A	B	ρ
Zero (No.1)	75.171	-91.383	0.998
No.1	64.731	-77.112	0.996
VII	75.958	-87.920	0.998
VIII	58.479	-64.894	0.992
IX	78.422	-92.697	0.999
X	75.520	-88.682	0.997
XI	88.890	-107.615	0.997
XII	80.410	-95.591	0.997
XIII	82.050	-96.447	0.995
XV	77.210	-92.395	0.998
XVI	85.200	-101.182	0.995
XVII	93.300	-111.297	0.993
XVIII	90.130	-108.422	0.998

Table 1: Linear fit values for the ash and specific gravity curve.

chosen and when half of the points were chosen. The pattern looked to be almost similar. It was therefore confirmed that the number of borehole points could be reduced in order to save the expenditure. In order to estimate/predict the values of these properties in coalfield a 3-D interpolation technique is employed. This is done using finite element method using AVS package. Fig. 2.7 shows the top and bottom seams of the Ghonsa coalfield with red indicating the highest sulphur content and the blue the lowest. The pointer shown in red points in three dimension at a point on the coalfield which gives the values of the sulphur content at that (x,y,z) point. This is validated with additional data set obtained from CFRI, Nagpur unit and was found to be predicting the values of the ash content, moisture, sulphur content etc., close to the observed value with a 90% confidence. With these values, one could obtain an overall estimate of the ash content, sulphur content etc. in the coalfield with minimum number of borehole points. *(N. K. Indira)*

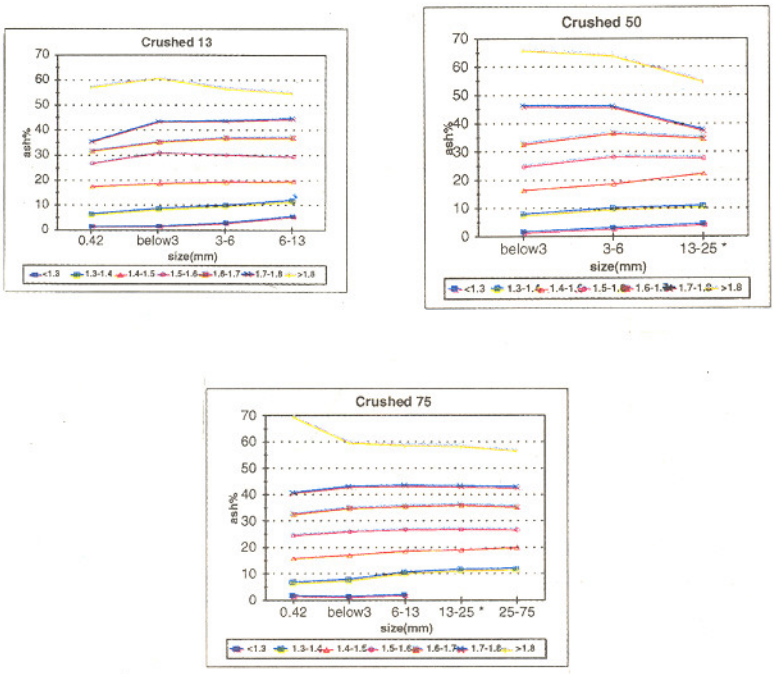

Fig. 2.7: Ash content versus size showing no change in the ash content due to size reduction. This is shown here for all the three cases of initial crushed coal of 13 mm, 50 mm and 75 mm.

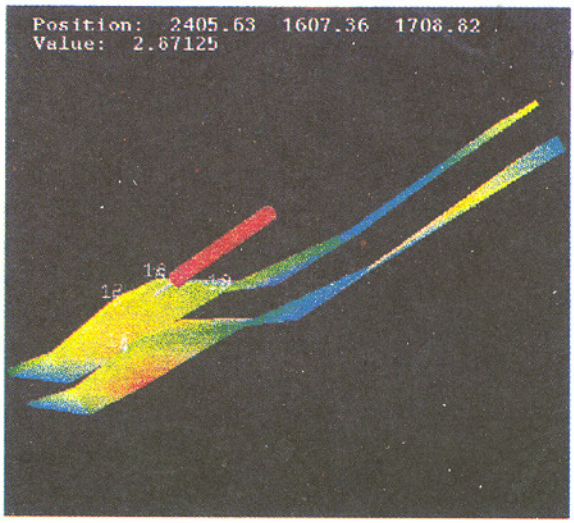

Fig. 2.8: Seam with both top and bottom section of Ghonsa coalfield indicating sulphur content.